Full Text View

Volume 30, Issue 11 (November 2000)

Journal of Physical Oceanography
Article: pp. 2637–2649 | Abstract | PDF (420K)

On the Propagation of Baroclinic Waves in the General Circulation

William K. Dewar

Department of Oceanography and Supercomputer Computations Research Institute, The Florida State University, Tallahassee, Florida

Michele Y. Morris

Centre for Atmospheric and Climatic Research, National Institute for Water and Atmospheric Research, Kilbirnie, Wellington, New Zealand

(Manuscript received March 9, 1999, in final form November 23, 1999)

DOI: 10.1175/1520-0485(2000)030<2637:OTPOBW>2.0.CO;2

ABSTRACT

The propagation of long, first mode, baroclinic planetary waves in eddy-resolving quasigeostrophic general circulation models is studied. Recent TOPEX/Poseidon observations argue oceanic first-mode planetary waves move with speeds other than those predicted by simple theory. These data have prompted theoretical analyses of wave propagation in a mean flow, with the results suggesting mean shear can have a controlling effect on the planetary wave guide. Some of the predicted effects appear to be relevant to the observations, while others are less obvious. This, coupled with other explanations for the observations, motivates the calculations.

Based on these experiments, the authors suggest that the predicted effects of mean shear on wave propagation are consistent with those computed in a fully geostrophically turbulent ocean. These are that a two-layer model misses the dominant component of long-wave interaction with a mean flow, a three-layer model captures this interaction qualitatively, and the correction to wave propagation is in the direction opposite to the mean flow. Quantitative comparisons between the theory and the numerical experiments are good in the northern latitudes and questionable in the southern latitudes. Reasons for the southern discrepancy are offered.

1. Introduction

Recently, Chelton and Schlax (1996, CS hereafter) have argued from TOPEX/Poseidon observations that 1) propagating sea surface height anomalies represented first-mode baroclinic waves and 2) those waves were moving at speeds

significantly different from the speeds predicted by the simplest linear wave theory. Higher latitude waves appeared to move faster than expected, while more equatorward waves were, if anything, slower. As baroclinic waves affect decadal ocean adjustment, their propagation is of importance to climate. Thus, the study of long baroclinic wave propagation is strongly motivated.

The objective of this study is to examine long, baroclinic planetary waves in the near-annual band in an eddy-resolving general circulation model. We test recent predictions of how these waves should be affected by mean flow. These predictions were derived using analytically tractable approximations to the quasigeostrophic equations. Here, numerical simulations using the full quasigeostrophic equations are studied.

a. Background

The theory of planetary waves dates to Hough (1897) and was advanced by Rossby (1940). Many investigators have described planetary waves in in situ ocean data (Bernstein and White 1974, 1977; Emery and Magaard 1976; Kang and Magaard 1980; Price and Magaard 1980, 1983, 1986; Sturges and Hong 1995; Sturges et al. 1998). Kang and Magaard (1980) and Price and Magaard (1983) found that accounting for mean shear improved planetary wave fits to their data. Kessler (1990) found in North Pacific XBT data a systematic tendency for linear wave theory to underpredict the observed wave speeds in the extratropical thermocline. The TOPEX/Poseidon analyses of CS, LeTraon and Minster (1993), and Cipollini et al. (1997) are consistent with the Kessler results and extend them to all the ocean basins. Morris (1996), in a quasigeostrophic numerical study of the South Pacific, found that the waves in her model moved at rates other than those predicted by either simple linear or two-layer theory. Thus, it appears that the simplest linear theories are an inaccurate model of oceanic planetary wave propagation.

This has generated considerable interest among theoreticians. Killworth et al. (1997) revisited the augmented eigenvalue problem using the Levitus dataset (Levitus 1982) and found that interaction of long waves with mean shear could account for much of the observed wave speed modification. Dewar (1998) looked at a global analysis of the large-scale quasigeostrophic equations and arrived at a similar result. The latter study also included an analytical expression for the mean flow effect on wave propagation and an explanation for why such results occurred within anticyclonic gyres.

Both above studies explained the so-called “non-Doppler” effect (Held 1983), that is, the result that long planetary waves in a one-layer reduced-gravity model are largely unaffected by mean flow, as due to the noninteraction of first-mode waves with the first mode of the mean flow. Dewar (1998) also argued that an anticyclonic stratified mean circulation should perturb the expected westward wave propagation cyclonically, that is, accelerate waves to the west in the northern half basin and slow them in the south. Liu (1999) found a similar result using ray tracing methods. The former tendency appears in the TOPEX/Poseidon results; the latter is much less clear.

These theories therefore appear to be relevant to the ocean, although questions remain. One possible explanation for the theory/observation mismatches is that the analyses are based in large-scale equations and miss some of the dynamics affecting wave propagation. Given this, the presence of different explanations for the CS observations [White et al. (1998) suggest air–sea coupling and Qiu et al. (1997) wind forcing, dissipation, and spatial resonance] and that the wave speed signals themselves are questioned (Zhang and Wunsch 1999), we feel it is useful to examine wave propagation in the presence of more complete physics. Testing the unobserved but predicted slowdown of waves in the south is also important for, if it is robust, the reason it is not observed becomes of interest.

We here test the above wave–mean flow theories using an eddy resolving quasigeostrophic (QG) general circulation model. Accordingly, we find the analytical model generally yields accurate qualitative predictions. A two-layer model yields a different wave propagation character than a three-layer model. Further, the Dewar (1998) estimates of enhanced long-wave propagation in the northern half of the subtropical gyre are quantitatively accurate. In the southern gyre half, where waves are predicted to slow, the full QG model yields relatively slow waves (although the predicted and computed speeds do not compare well). A many-layer model does not differ significantly from the three-layer model in wave propagation, arguing that a three-layer model is adequate for process studies. Propagation in inertial recirculations is not well captured by the theory.

The theory of long wave–mean flow interaction using large-scale quasi-geostrophic theory is briefly reviewed in the next section. Section 3 describes our numerical design and the results of our experiments. A discussion section concludes the paper.

2. Long wave–mean flow interaction theory

The inviscid QG potential vorticity equations for a three-layer system are

$$\frac{\partial}{\partial t} q_1 + J(\psi_1, q_1) = \frac{w_e}{H_1},$$

$$q_1 = \nabla^2 \psi_1 - \frac{f_o}{H_1} h_1 + \beta y$$

$$\frac{\partial}{\partial t} q_2 + J(\psi_2, q_2) = 0;$$

$$q_2 = \nabla^2 \psi_2 + \frac{f_o}{H_2}(h_1 - h_2) + \beta y$$

$$\frac{\partial}{\partial t} q_3 + J(\psi_3, q_3) = 0;$$

$$q_3 = \nabla^2 \psi_3 + \frac{f_o}{H_3} h_2 + \beta y, \qquad (1)$$

where β is the north–south gradient of the Coriolis parameter, $f = f_o + \beta y$, q_i denotes the potential vorticity of layer i, ψ_i the streamfunction for layer i, h_i the interface perturbation for the interface between layers i and $i + 1$, and w_e is the Ekman pumping at the surface. Interface perturbations are related to streamfunctions via

$$g_i' h_i = f_o(\psi_i - \psi_{i+1}), \qquad (2)$$

where g_i' is the reduced-gravity parameter of interface i. A schematic of the model appears in Fig. 1.

The large-scale QG (LSQG) equations are obtained from (1) by neglecting relative vorticity, which reduces potential vorticity to contributions from β and vortex tube stretching. The analysis in Dewar (1998) can be replicated by linearizing the LSQG about a mean flow, the structure of which is straightforward to extract from the steady LSQG. These linearized equations can be rewritten in terms of the linear normal modes, $h_\pm$, denoting the first and second baroclinic modes of the system. We will make three further, nonessential but algebraically convenient, assumptions: first, the third layer is assumed very deep and thus has negligible velocities; second, $H_1 = H_2$; and third, $g_1' = g_2'$.

The resulting first-mode wave equation is

$$\frac{\partial}{\partial t} h_+ + J\left(\frac{g'}{f_o} \frac{h_{o-}}{(\alpha_- - \alpha_+)} + \beta_+ y,\ h_+\right)$$

$$= -(1 - \alpha_+) w_e' + J\left(\frac{g'}{f_o} \frac{h_{o+}}{\alpha_- - \alpha_+},\ h_-\right), \qquad (3)$$

where w_e' denotes the time dependent part of wind forcing and

$$\beta_\pm = \frac{\beta g_1' H_1}{f_o^2}(1 - \alpha_\pm), \qquad (4)$$

where $\alpha_\pm$ is an eigenvalue. The quantities $\beta_\pm$ denote the first- and second-mode wave speed and $h_{o\pm}$ the projections of the mean state onto the first and second baroclinic normal modes.

Comparing first- and second-mode speeds in (4) reveals that the second mode is typically slower than the first mode. (This is characteristic of oceanic stratifications.) Therefore, near-annual frequencies in forcing, like those studied by CS, generate short second-mode waves relative to the first-mode waves. Dewar (1998) argued by spatial averaging that the underlined Jacobian on the right-hand side of (3) can be ignored, even though the ratio of the wave lengths is not very small ($\approx 1/6$). The result is a closed equation for the first baroclinic long-wave mode propagating in the presence of a mean flow. In view of the uncomfortably weak scale separation, however, the equation can be criticized.

It is seen from (3) that the second mode of the general circulation, h_{o-}, affects the first-mode wave propagation. This is the appearance in this problem of the "non-Doppler" effect. Had this same analysis been conducted in a "1½" layer model, h_{o-} in (3) would not appear and the first-mode wave would propagate as if no mean flow were present.

If the third layer is finite, the upper two layers have arbitrary thicknesses, and the g_i' are not identical, as will characterize the numerical solutions discussed later, (3) generalizes to

$$h_{+t} + J\left(\frac{\phi}{H} + \frac{\beta g_1' H_1}{f_o^2}\Delta y - \left(\frac{H_3}{H} - \frac{\alpha_+ \gamma H_1}{H}\right)\frac{H_3\gamma}{df_o H}h_{o-}, h_+\right)$$

$$= -\Delta w_e' - J\left(\frac{\phi}{H}, h_{o+}\right) \qquad (5)$$

where

$$\Delta = \frac{H_2 + H_3}{H} - \alpha_+ \frac{H_3}{H} \qquad (6)$$

$$d = \sqrt{\left((1+\lambda)\frac{H_3}{H} - \frac{\gamma(H_2+H_3)}{H}\right)^2 + 4\gamma\left(\frac{H_3}{H}\right)^2} \qquad (7)$$

$$\alpha_\pm = -\frac{H}{2H_3\gamma}\left[(1+\lambda)\frac{H_3}{H} - \gamma\left(\frac{H_2+H_3}{H}\right) \pm d\right], \qquad (8)$$

$\lambda = H_2/H_1$, and $\gamma = g_1'/g_2'$. The quantity Φ in (5) denotes the presence of the barotropic mode. This augments h_+ propagation by a Doppler shift and also affects the local h_+ production.

Generalizations to continuous stratification suggest higher mean field modes guide first-mode waves as in (5) but weaken in effect with increasing mode number. Equation (5) constitutes the approximate theory we test in the next section.

3. Numerical experiments

a. Numerical model

We employ the Holland (1978) quasi-geostrophic model in a rectangular, flat bottom 3000 km by 2000 km basin. The grid resolution is 10 km in both directions and the total depth of the fluid is 5000 m. We have experimented with a variety of stratifications. Our main runs used a three-layer model with g_1' = 0.035 m s^{-2}, g_2' = 0.025 m s^{-2}, H_1 = 300 m, H_2 = 700 m, and H_3 = 4000 m, resulting in first and second deformation radii of 52.3 km and 26.8 km. The first mode is relatively well resolved, while the second mode is poorly resolved, but present. We have also run two-layer and six-layer experiments. In the former, g_1' = 0.024 m s^{-2} and H_1 = 1000 m were used to match the first baroclinic deformation radius from the three-layer experiment. This assured that the simplest first baroclinic wave speeds were identical in these experiments. For the six-layer experiment, we matched the first and second deformation radii. This was deemed necessary as the previous theory emphasized the role of the second mean flow mode in modifying first-mode planetary wave speeds. Clearly, the

parameters meeting this condition are not unique. The six-layer experiment used reduced gravity paramaters of 0.025, 0.025, 0.0141, 0.0036, and 0.005 84 m s^{-2} and thicknesses of 250 m, 250 m, 250 m, 250 m, 2000 m, and 2000 m. These yielded first and second deformation radii identical to the three-layer run to four digits.

In all experiments, $f_o = 0.93 \times 10^{-4}$ s^{-1} and $\beta = 2 \times 10^{-11}(\text{m s})^{-1}$. Laplacian viscosity was used with coefficient 300 m^2 s^{-1}. No-slip boundary conditions were employed to keep inertial recirculations from becoming larger than desired.

We focus on subtropical gyres as the relevant CS results come mostly from subtropical latitudes. We therefore forced the model with the time-dependent subtropical gyre Ekman pumping

$$w_e = -1.7 \times 10^{-6}[1 + 0.5\sin(\omega t)]\sin\left(\pi\frac{y}{L}\right) \ [\text{m s}^{-1}], \tag{9}$$

where L is the meridional basin length. We have studied mostly annual and biannual forcings.

It was found that the amplitude of the waves generated by the Holland model were 10 times larger than those predicted by our theory. The reason for this is that the streamfunction values on the boundaries must be computed for the quasigeostrophic equations (McWilliams 1977). This gives the full QG equations a way to generate waves that has no analog in (5). Fortunately, this does not impact our comparisons because we are interested in the propagation within the domain. We do note, however, that the “large” first-mode waves in the Holland model test the viability of (5) well into the quasigeostrophic nonlinear regime.

All runs were spun up for approximately 40 years using the mean wind profile only. The model by then exhibited at most weak trends, so the variable part of the Ekman pumping was engaged, and the models were run for an additional 20 years. Here, we show results of the model averaged over the last several years.

b. Three-layer runs

In Figs. 2a,b, we show the mean first- and second-layer streamfunctions averaged over the last 12 years of our standard three-layer run. The structure of the mean flow consists of a western boundary current, a Sverdrup interior, and an inertial recirculation confined in the northwestern basin corner. The interior transport is roughly 20 Sv (Sv $\equiv 10^6$ m^3 s^{-1}) and the recirculation is about 50 Sv. The former number is representative, if a bit weak, of the North Atlantic and Pacific interior transports; the latter is somewhat weaker than the observed inertial recirculations. Figure 2c shows the distribution of the upper layer eddy kinetic energy averaged over the last 12 years of our run. Maximum eddy kinetic energies occur in the vicinity of the western boundary current eastward extension with a secondary maximum located in the western return flow of the gyre. Typical rms eddy velocities in the upper layer are on the order of 0.3–0.5 m s^{-1}. In all, the circulation is a useful idealization of the real ocean.

1) BASINWIDE COMPARISONS

In Fig. 3, we show four snapshots of the first baroclinic mode amplitude from the three-layer model. This plot was generated by first subtracting mean fields, shown in Figs. 2a,b, from archived output fields. The residuals were then projected onto the first mode according to $h_+ = h_1 - \alpha_+ h_2$, with α_+ defined by (8). The four snapshots in Fig. 3 come at quarter cycles of the forcing: Fig. 3a is at the maximum wind amplitude, Fig. 3b three months later, Fig. 3c at the minimum wind amplitude, and Fig. 3d three months later. Results at these fixed phases from 12 years of model output were averaged to reduce the eddy noise. Note the tendency for the wave fronts to tilt cyclonically as one moves from the eastern boundary toward the western basin edge.

In Fig. 4, we show the solution of (5), the simplified first-mode propagation equation including the mean flow, for the same wind forcing as was used to generate Fig. 3. Here we have used the mean fields shown in Fig. 2 to determine the mean-shear contribution to the wave propagation. The solution computed using (5) contains no eddies and is much more spatially regular. The overall pattern of the wave amplitude computed from the simplified theory, however, qualitatively matches that of the full QG model in Fig. 3 quite well.

2) TIME–LONGITUDE PLOTS: STRENGTHS AND WEAKNESSES

Figures 5 and 6 show time–longitude plots of the first baroclinic mode amplitudes. These plots correspond to latitudes 500 km and 1400 km north of the southern basin boundary and only the eastern 2200 km are shown to avoid the western boundary current. The data were zonally averaged and the average removed to emphasize the propagating waves relative to the stationary effect of the pumping. Results at fixed phases from 12 years of model output were averaged to remove noise.

In the upper plot in Fig. 5a, we compare propagation from the full QG model with a mean flow (solid lines) to propagation from the full QG model forced only by the variable part of the Ekman pumping (dashed lines). Thus, the latter waves move in the absence of a mean flow and exhibit simple nondispersive propagation, as seen from the nearly straight contours (dashed lines). (The waviness in these contours is due to time dependent barotropic Doppler shifting.) Relative to these almost straight lines, the waves from the fully forced model begin in the east as simple waves, but by midbasin are accelerating relative to the background speed. This is in qualitative agreement with our theoretical expectations. The same information appears in Fig. 5b, except results from the simple analytical model in (5) appear as dashed lines in place of those from full QG model. The solid lines are still from the Holland QG model without a mean flow. Note that this plot is quite similar to Fig. 5a, suggesting that the qualitative character of wave propagation in the general circulation has been captured by the simple analytical theory. Fig. 5c shows the quantitative comparison is also favorable, as we directly compare results from (5), contoured in dashed lines, to results from the fully forced QG model (solid lines). Comparable westward acceleration of the pattern propagation with increasing distance from the eastern boundary is clear in all three plots.

Figure 6 compares the same three models at the more southerly latitude Y = 500 km. The presentation is as in Fig. 5. The quantitative comparison at this latitude between the various models is not as good as at Y = 1400 km. In the southern part of the domain, the wave–mean flow effect is expected to retard wave propagation. This appears in the lagging of the solid-line contours (QG with mean flow) relative to the dashed-line contours (QG no mean flow) noted in midbasin in Fig. 6a. This comparison is consistent with the theoretically expected tendency. However, the comparison in Fig. 6b of the analytical predictions (dashed) against the full numerical model without a mean flow (solid) reveals at best a weak effect. There is a slight lagging of the analytical contours relative to the computed contours in midbasin, but the difference is considerably less than appears in Fig. 6a. Comparisons of the full QG model results (solid) to those generated by (5) (dashed) at Y = 500 km are in Fig. 6c. As expected from Fig. 6b, (5) is less successful as a quantitative model of wave propagation.

The reasons for this are not clear, but possibly involve wave dispersion. Note in Fig. 4 that this latitude is characterized by the appearance of relatively small scales in the wave pattern. Some of these reflect smaller scales in the mean circulation, some the slant in wave amplitudes caused by wave speed variations and some the slower wave phase speeds themselves. Dispersion should slow down a wave according to full quasigeostrophic theory, and this is in keeping with the comparison between the analytically expected result and the full result. It is also possible that the smaller scales appearing in the south elevate the underlined Jacobian in (3) in magnitude. This would weaken the quantitative skill of the theory although it is not clear that the Jacobian should have the observed effect. It is still true that the qualitative slowing of the waves in the south, appearing in the full QG solutions, is captured by the approximate equation in (5).

The predictions from (5) also lose accuracy as the waves move into the inertial recirculations, suggesting that the simple theory does not work well there. The limitations on the size and strength of the inertial recirculations in these runs has prevented us from studying this area more fully; further work is necessary.

c. Two-layer runs

Figure 7 shows essentially the same plan view as Fig. 3; however the output comes from a two layer QG model. Aside from this, the runs use the same grid resolution, viscosity, wind forcing, etc., as the three-layer model. It is nonetheless clear that the propagating wave crests behave very differently. The cyclonic tendency seen in Fig. 3 for the wave crests is replaced by an anticyclonic correction. The latter is due to the Doppler shift caused by the depth integrated Sverdrup flow, which for a subtropical gyre is anticyclonic. Dewar (1998) argues this effect is inversely proportional to the total depth of the water column. Thus, this term is absent in (3) because of the very deep third layer, but appears in (5). The numerical run shown in Fig. 7 has a finite total depth of 5000 m, yielding a measurable Doppler shift of $\leqslant 1$ cm s^{-1}. This agrees with the results in Fig. 7 and also with differences between integrations of (3) and (5) (not shown).

The comparison between Figs. 3 and 7 supports the prediction that a two-layer model misses leading order wave–mean shear interaction physics. This interaction dominates the Doppler shift, as supported by the net cyclonic correction in Fig. 3. Recall that that experiment also had a depth of 5000 m, so the anticyclonic Doppler effect was the same strength as in Fig. 7.

d. Six-layer runs

We show in Fig. 8 the results of a six-layer experiment. The purpose here was to test the prediction that a three-layer model captures the dynamics of wave–mean flow interaction both qualitatively and quantitatively. The same format as Fig. 3 is used. Note that the plot is considerably noisier. This reflects the enhanced eddy activity typical of more highly stratified layered model experiments. Aside from that, the correspondence in plan view of the wave crests is quite good. The overall correction to the crest structure is cyclonic and of approximately the same amplitude as that in the three-layer experiment. The propagation speed of the first-mode waves is also roughly the same in both figures, as is evidenced by the positioning of the wave crests relative to the eastern basin boundary at the various phases of the forcing cycle.

This correspondence is emphasized in Fig. 9, which compares time–longitude plots from the three- (solid) and six- (dashed) layer runs at the latitudes of Y = 1400 km and 500 km. Here again the zonal average of the data has been removed to accentuate signal propagation. We expect acceleration of the wave signal in the northern transect and deceleration in the southern. Both signals are observed and, further, the comparison of the first-mode propagations is surprisingly good, supporting the quantitative accuracy of the three-layer model.

It is key here that both the first and second baroclinic deformation radii have been matched. In other experiments (not shown here), the quantitative behavior of the first-mode propagation was captured when only the first deformation radius was matched, but the quantitative comparison was degraded. This reflects that the mean flow effect on the waves depends on the second general circulation mode.

4. Discussion

An eddy resolving quasigeostrophic numerical model was used to study first-mode long planetary wave propagation in the presence of mean flow. Previous theoretical studies have argued that long-wave propagation in a flat bottom ocean is due to β (which generates simple westward propagation), a Doppler shift by the barotropic flow, and an interaction with the mean shear profile. The latter has been argued to be insensitive to the representation of stratification in a model; the minimal requirements are that the first two internal deformation radii be accurately represented. All of the above points are supported in this study.

Relative to observations, such as those in CS, wave crests are accelerated in their westward propagation in the northern part of the subtropical gyre and decelerated in the southern part. The northern model tendency appears in CS. While tropical latitudes yielded different wave behaviors (the waves moved slower than expected), comparison with CS is less satisfactory. On the other hand, detailed comparison between the observations and the model is ambiguous in the near-equatorial regions. The equatorial mean flow field is not captured by our subtropical gyre model. Further, QG dynamics ignore the explicit variation of the Coriolis parameter, thus neglecting the phase speed growth of long waves in the equatorial zone. In our opinion, these QG shortcomings recommend caution when applying this theory to the equatorial ocean regime and call for a closer examination of long-wave propagation using planetary geostrophic equations. The latter supercede QG and include the explicit variation of the Coriolis parameter.

We have also noted tendencies for the theory to be inaccurate in the inertial recirculation zones of the model and for the quantitative fidelity of the theory to degrade in the southern half of the domain. In a sense, the former is not a surprise, as the LSQG equations do not capture the dynamics of the recirculation. A more thorough study of long-wave propagation in the presence of an inertial recirculation is called for. The latter possibly reflects dispersion.

In closing, three further points deserve explicit mention. First, ours is an ocean-only model; yet, we predict modifications to wave propagation consistent with the CS observations. The coupled dynamics shown recently by White et al. (1998) to cause westward wave acceleration may occur in the real ocean, but our calculations show other dynamics internal to the ocean may play a comparable role.

Second, Qiu et al. (1997) show how the phase speed doubling, first noticed by White (1977), is made more apparent in the off-equatorial bands by dissipation. Specifically, pattern speed doubling is accompanied by intervals of vanishing pattern propagation due to interference between local and propagating effects. Dissipation damps the propagating part, allowing the locally forced, faster component to dominate in the interior. Shorter waves, naturally occurring at higher latitudes, are more efficiently damped, generating a signal like that in CS. Our eddy-resolving runs, in principle, explicitly model the dissipative mechanisms parameterized by Qiu et al. (1997) and wavelengths of our generated waves are like those noted by CS in the extratropical zones. Our results thus suggest eddy-resolving models do not necessarily strongly damp propagative waves. Our averaging procedure also removes the spatially fixed part of the solution, thereby emphasizing the propagative wave. The computed acceleration of the motion is thus a property of wave–mean flow interaction, and not of spatial resonance. We feel wave–mean flow interaction should not be discounted relative to the mechanics suggested by Qiu et al. (1997).

Third, these results comment on the minimal model required to study climate and climate variability, and there is good news and bad news. Oceanic adjustment on the largest scales is undoubtedly mediated via first-mode baroclinic waves. Further, the climate is complex, so it is rational to construct minimal models to gain insight. The bad news is that to capture

the basic mechanics by which the ocean adjusts to variability requires at least three layers, rather than the computationally less demanding two-layer system. The good news is that for process climate ocean modeling, more than three layers may well be “gilding the lily.”

Acknowledgments

The authors would like to acknowledge many interesting discussions on this work with R. X. Huang. WKD is supported through NSF Grant OCE-9617728 and NASA Grant NAG5-7630. Sheila Derby aided in manuscript and figure preparation and Jane Jimeian assisted with many computational issues.

REFERENCES

Bernstein, B., and W. White, 1974: Time and length scales of baroclinic eddies in the central North Pacific Ocean. *J. Phys. Oceanogr.*, **4,** 123–126. Find this article online

— ,and — ,1977: Zonal variability in the distribution of eddy energy in the mid-latitude North Pacific Ocean. *J. Phys. Oceanogr.*, **7,** 123–126. Find this article online

Chelton, D., and M. Schlax, 1996: Global observations of oceanic Rossby waves. *Science*, **272,** 234–238.

Cipollini, P., M. Cromwell, G. Quartly, and P. Challenor, 1997: Concurrent altimeter and infrared observation of Rossby wave propagation near 34°N in the northeast Atlantic. *Geophys. Res. Lett.*, **24,** 889–892.

Dewar, W., 1998: On too-fast baroclinic planetary waves in the general circulation. *J. Phys. Oceanogr.*, **28,** 1739–1758. Find this article online

Emery, W., and L. Magaard, 1976: Baroclinic Rossby waves as inferred from temperature fluctuation in the eastern Pacific. *J. Mar. Res.*, **34,** 365–385.

Held, I., 1983: Stationary and quasi-stationary eddies in the extra-tropical troposphere: Theory. *Large-Scale Dynamical Processes in the Atmosphere*, P. Hoskins and R. Pierce, Eds., Academic Press, 127–168.

Holland, W., 1978: The role of mesoscale eddies in the general circulation of the ocean—Numerical experiments using a wind-driven quasi-geostrophic model. *J. Phys. Oceanogr.*, **8,** 363–392. Find this article online

Hough, S., 1897: On the application of harmonic analysis to the dynamical theory of the tides, Part I. On Laplace’s “oscillations of the first species,” and on the dynamics of ocean currents. *Philos. Trans. Roy. Soc. London*, **189A,** 201–257.

Kang, Q., and L. Magaard, 1980: Annual baroclinic Rossby waves in the central North Pacific. *J. Phys. Oceanogr.*, **10,** 1156–1167. Find this article online

Kessler, W., 1990: Observations of long Rossby waves in the northern tropical Pacific. *J. Geophys. Res.*, **95,** 5183–5218.

Killworth, P., R. DeSzoeke, and D. Chelton, 1997: The speed of observed and theoretical long extratropical planetary waves. *J. Phys. Oceanogr.*, **27,** 1946–1966. Find this article online

Le Traon, P., and J. Minster, 1993: Sea level variability and semiannual Rossby waves in the South Atlantic subtropical gyre. *J. Geophys. Res.*, **98,** 12 315–12 326.

Levitus, S., 1982: *Climatological Atlas of the World Ocean.* NOAA Prof. Paper No. 13, U.S. Govt. Printing Office, 173 pp.

Liu, Z., 1999: Planetary wave modes in the thermocline: Non-Doppler-shift mode, advective mode and Green mode. *Quart. J. Roy. Meteor. Soc.*, **125,** 1315–1339.

McWilliams, J., 1977: A note on a consistent quasigeostrophic model in a multiply connected domain. *Dyn. Atmos. Oceans*, **1,** 427–441.

Morris, M., 1996: Mean and low frequency fluctuations in the circulation of the western/central Pacific Ocean. Ph.D. thesis, University of California, San Diego–Scripps Institute of Oceanography, 203 pp.

Price, J., and L. Magaard, 1980: Rossby wave analysis of the baroclinic potential energy in the upper 500 meters of the North Pacific. *J. Mar. Res.*, **38,** 249–264.

— ,and — ,1983: Rossby wave analysis of subsurface temperature fluctuations along the Honolulu–San Francisco great circle. *J.*

Phys. Oceanogr., **13,** 258–268. Find this article online

— ,and — ,1986: Interannual baroclinic Rossby waves in the midlatitude North Atlantic. *J. Phys. Oceanogr.*, **16,** 2061–2070. Find this article online

Qiu, B., W. Miao, and P. Mueller, 1997: Propagation and decay of forced and free baroclinic Rossby waves in off-equatorial oceans. *J. Phys. Oceanogr.*, **27,** 2405–2417. Find this article online

Rossby, C., 1940: Planetary flow patterns in the atmosphere. *Quart. J. Roy. Meteor. Soc.*, **66**(Suppl.), 68–97.

Sturges, W., and B. Hong, 1995: Wind forcing of the Atlantic thermocline along 32°N and low frequencies. *J. Phys. Oceanogr.*, **25,** 1706–1715. Find this article online

— ,— ,and A. Clarke, 1998: Decadal wind forcing of the North Atlantic subtropical gyre. *J. Phys. Oceanogr.*, **28,** 659–668. Find this article online

White, W., 1977: Annual forcing of baroclinic long waves in the tropical North Pacific. *J. Phys. Oceanogr.*, **7,** 50–61. Find this article online

— ,Y. Chao, and C.-K. Tai, 1998: Coupling of biennial oceanic Rossby waves with the overlying atmosphere in the Pacific basin. *J. Phys. Oceanogr.*, **28,** 1236–1251. Find this article online

Zhang, X., and C. Wunsch, 1999: The observed dispersion relationship for North Pacific Rossby wave motions. *J. Phys. Oceanogr.*, **29,** 2183–2190. Find this article online

---

Figures

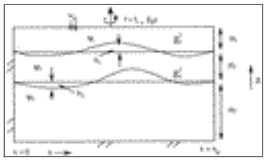

Click on thumbnail for full-sized image.

Fig. 1. A three-layer configuration is shown. The model is flat bottomed, forced by a variable wind, and on a β plane. Notation is standard

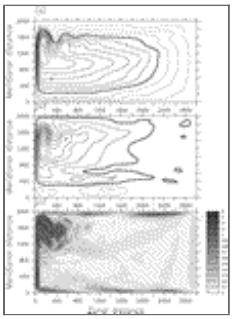

Click on thumbnail for full-sized image.

Fig. 2. Mean state circulation: (a) upper-layer streamfunction averaged over the last 12 years of our three-layer experiment (units are 103 m^2 s^{-1}); (b) second-layer streamfunction, so averaged (units are 103 m^2 s^{-1}); (c) eddy kinetic energy from the upper layer, so averaged (units are m^2 s^{-2})

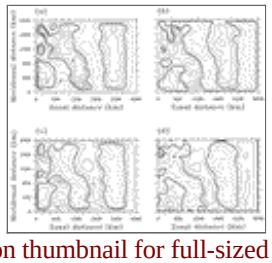

Click on thumbnail for full-sized image.

Fig. 3. First baroclinic mode wave propagation at fixed phases, and averaged over the last 12 years of our three-layer

experiment: (a) at the point of maximum Ekman pumping, (b) three months later than (a), (c) at the point of minimum Ekman pumping, and (d) three months later than (c)

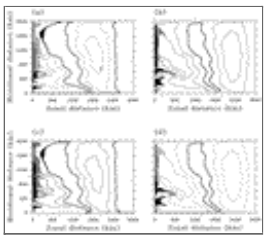

Click on thumbnail for full-sized image.

Fig. 4. As in Fig. 3 but using the asymptotic theory in (5)

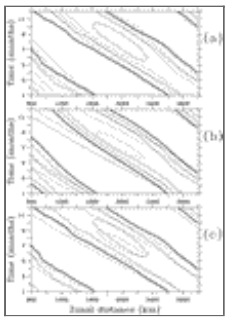

Click on thumbnail for full-sized image.

Fig. 5. Time–longitude plots: (a) wave propagation in the presence of mean flow (solid) is compared to propagation in the absence of mean flow (dashed). Both were computed using the full QG model. $Y = 1400$ km. (b) Wave propagation from the analytical theory (dashed) compared to propagation from the full QG model without mean flow (solid); $Y = 1400$ km. (c) Wave propagation from the analytical theory (dashed) compared to propagation from the full QG model with mean flow (solid); $Y = 1400$ km. The zonal average of the data has been removed in all cases

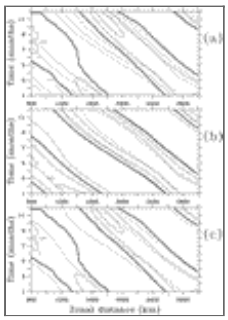

Click on thumbnail for full-sized image.

Fig. 6. As in Fig. 5 but at $Y = 500$ km

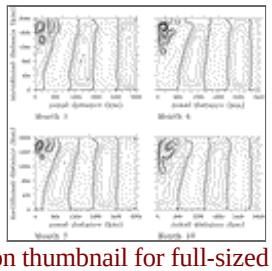

Click on thumbnail for full-sized image.

Fig. 7. As in Fig. 3 but using a two-layer QG model

Click on thumbnail for full-sized image.

Fig. 8. As in Fig. 3 but using a six-layer QG model

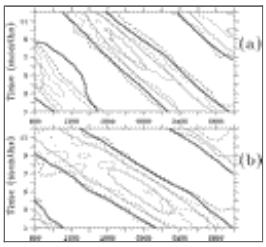

Click on thumbnail for full-sized image.

Fig. 9. Time–longitude plots comparing the three-layer model (solid) to the six-layer model (dashed): (a) Y = 500 km and (b) Y = 1400 km. The zonal average of the data has been removed

Corresponding author address: Dr. William K. Dewar, Dept. of Oceanography, The Florida State University, Tallahassee, FL 32306-4320.
E-mail: dewar@ocean.fsu.edu

top